Heliyon 10 (2024) e24239

Contents lists available at ScienceDirect

Heliyon

journal homepage: www.cell.com/heliyon

Research article

Proteins extracted from pearl oyster (*Pinctada martensii*) with efficient accelerated wound healing in vitro through promoting cell proliferation, migration, and collagen formation

Tao Zeng [a,b,1], Lianfeng Liu [a,d,1], Dandan Mo [a,b], Qinghua Yang [a,e], Xiaohao Hu [a,b], Chun Lu [f], Ran Sun [a,b], Li Zheng [a,b,**], Bo Zhou [a,b,***], Sheng Xu [a,b,c,*]

[a] *Collaborative Innovation Centre of Regenerative Medicine and Medical Bioresource Development and Application Co-constructed by the Province and Ministry, The First Affiliated Hospital of Guangxi Medical University, Nanning, 530021, China*
[b] *Guangxi Engineering Center in Biomedical Materials for Tissue and Organ Regeneration, The First Affiliated Hospital of Guangxi Medical University, Nanning, 530021, China*
[c] *Life Sciences Institute, Guangxi Medical University, Nanning, 530021, China*
[d] *Department of Ultrasound, Guangxi Medical University Cancer Hospital, Nanning, 530021, China*
[e] *Department of Orthopedics, The First Affiliated Hospital of Guangxi Medical University, Nanning, 530021, China*
[f] *School of Materials and Environment, Guangxi Minzu University, Nanning, Guangxi, 530006, China*

A B S T R A C T

Ethnopharmacological relevance: Pearl oyster (*Pinctada martensii*) is used in Chinese traditional medicine use in photoprotective, anti-inflammatory, and wound treatment.

Aim of the study: This study explored whether the mucus protein of Pearl oyster (protein of *Pinctada martensii*, PMP) affects human skin fibroblast (HSF) proliferation, migration, collagen-related gene expression related to collagen formation, and in vivo healing effects.

Materials and methods: The PMP component was analyzed by LC-MS/MS. The cell viability was evaluated using a CCK-8 kit. The expression genes were measured by reverse transcription polymerase chain reaction. A full-thickness excisional wounding model in Sprague-Dawley (SD) rats was used to test the repairing effect of PMP in vivo, and Hematoxylin-Eosin (H&E) and Masson's Trichrome staining were applied to evaluate skin structure.

Results: The components of PMP were identified using LC-MS/MS proteomics, and a total of 3023 proteins were detected. The results of PMP-treated HSF showed that PMP effectively promoted cell proliferation by 1.6-fold and cell migration by 1.5-fold at a concentration of 1 mg/mL. Additionally, PMP treatment up-regulated the expression levels of collagen-related genes COL1A1, COL3A1, and MMP-1 in fibroblasts. Furthermore, PMP was applied in the therapy of full-thickness excisional wounds in rats. The results demonstrated that PMP significantly accelerated wound healing time, resulted in the recovery of dermal and epithelial thickness, and stimulated collagen regeneration. The regenerated skin closely resembled the structure of normal skin.

Conclusions: These findings provide solid evidence supporting the potential of PMP as a promising candidate for the treatment of skin wounds.

* Corresponding author. Collaborative Innovation Centre of Regenerative Medicine and Medical Bioresource Development and Application Co-constructed by the Province and Ministry, The First Affiliated Hospital of Guangxi Medical University, Nanning, 530021, China.

** Corresponding author. Collaborative Innovation Centre of Regenerative Medicine and Medical Bioresource Development and Application Co-constructed by the Province and Ministry, The First Affiliated Hospital of Guangxi Medical University, Nanning, 530021, China.

*** Corresponding author. Collaborative Innovation Centre of Regenerative Medicine and Medical Bioresource Development and Application Co-constructed by the Province and Ministry, The First Affiliated Hospital of Guangxi Medical University, Nanning, 530021, China.

E-mail addresses: zhengli224@163.com (L. Zheng), gxzhoubo520@126.com (B. Zhou), xusheng@gxmu.edu.cn (S. Xu).

[1] These authors contributed equally.

https://doi.org/10.1016/j.heliyon.2024.e24239
Received 26 June 2023; Received in revised form 4 January 2024; Accepted 4 January 2024
Available online 6 January 2024

1. Introduction

The *Pinctada martensii*, commonly known as the pearl oyster, is a bivalve mollusk that is cultured in marine environments. Historical records from China dating back 2000 years mention the use of pearls in traditional medicine, with nine ethnic groups and 251 prescription formulations utilizing pearls as a medicinal material [1,2]. The *Pinctada martensii* have been found to possess various

Abbreviations

PMP	protein of *Pinctada martensii*
MMP-1	matrix metallopeptidase-1
bFGF	basic fibroblast growth factor
PDGF	platelet-derived growth factor
ECM	extracellular matrix
PM	*Pinctada martensii*
HSF	human skin fibroblasts
CCK-8	Cell Counting Kit-8
TLR	Toll-like receptor
PAMP	pathogen-associated molecular patterns
LC-MS/MS	Liquid Chromatography-Mass Spectrometry

biological activities, including sedation, cognitive enhancement, antiepileptic effects, promotion of bone growth and regeneration, and stimulation of cell proliferation. Previous studies have indicated that the process of pearl formation in *Pinctada martensii* begins with the secretion of pearl matrix by the mantle tissue, which then encapsulates foreign objects [3,4]. It is believed that the bioactive components found in pearls are closely associated with the mucous secretion produced by the mantle epithelial cells. These components include proteins, calcium carbonate, and other trace elements.

The skin serves as the body's primary line of defense in the immune system, protecting the organism from pathogens [5]. Trauma, which includes wounds caused by accidents, is a common skin condition. Treating these wounds quickly and effectively is crucial for survival in dangerous natural environments [6,7]. During the process of wound healing, fibroblast proliferation and migration play a critical role in the formation of new tissue. This includes steps such as angiogenesis, inflammation production, wound contraction, and tissue remodeling [8]. Fibroblasts secrete various factors, including matrix metallopeptidase-1 (MMP-1), basic fibroblast growth factor (bFGF), and platelet-derived growth factor (PDGF). These factors regulate collagen metabolism and angiogenesis to promote wound healing [9–11]. Additionally, the deposition produced by fibroblasts supports the formation of extracellular matrix (ECM) and provides an environment for the migration and proliferation of other cells [12]. Given the importance of fibroblasts in wound healing, it is clinically significant to explore effective methods that can promote fibroblast migration and proliferation [11]. Currently, epidermal growth factor and basic fibroblast growth factor are the main drugs used to promote fibroblast hyperplasia and treat wounds [13,14]. However, their short half-life, susceptibility to degradation, limited resources, and high cost hinder their wider application [15].

Biological and pharmacological activities of bioactive proteins and peptides derived from marine organisms have been extensively studied. In China, pearls have been traditionally used in medicine [16]. During the formation of pearls, a significant amount of mucus is produced, which may possess pharmacological effects. Mucus membranes found in various animals serve a protective function against the external environment and have been utilized for disease treatment and therapy.

For instance, catfish mucus exhibits potent antimicrobial properties [17], and researchers have developed antimicrobial peptide products derived from recombinant peptides found in catfish mucus [18]. The mucus of the amphibian *Rana chensinensis* also demonstrates multifunctional activity, protecting the frog's survival and promoting skin healing [19–21]. Snail mucus is another example that has been used in treating skin wounds and promoting skin whitening. It accelerates wound healing by facilitating cell proliferation and migration [22]. Considering these therapeutic benefits, animal mucus holds promise for treating skin damage [23,24]. *Pinctada martensii* (PM), a bivalve mollusk primarily cultivated in China and Japan, secretes a substantial amount of mucus during its growth and has garnered attention from researchers [25].

A large amount of mucus is secreted during the growth of PM, which has been made attention to by researchers. Previous studies have shown that enzyme products derived from PM meat and small molecular polypeptides from the mantle have promoted wound healing in rats, with amino acids and various peptides being the main components [26–29]. However, most of these studies have predominantly focused on PM peptides. Given that the proteome of PM undergoes significant changes during pearl production, we hypothesize that the changing proteins may possess excellent wound repair activity due to the protection mechanism of PM.

In this study, we extracted and purified a natural protein from PM, referred to as PMP (Protein of *Pinctada martensii*), using filtration and centrifugation techniques. The composition of PMP was then analyzed using LC-MS/MS. Through this analysis, we identified various proteins, including ATP synthase, RNA binding proteins, and other proteins known to promote cell growth. We conducted experiments to investigate the effects of PMP on HSF proliferation and migration. Our findings revealed that PMP significantly enhanced both HSF proliferation and migration. Furthermore, we examined gene expression changes in collagen I, collagen III, and MMP-1, which are essential for wound healing. We observed up-regulation of these genes upon treatment with PMP, suggesting its potential role in promoting wound repair. To further evaluate the wound healing properties of PMP, we utilized a rat skin wound

model in vivo (as shown in Scheme 1). Our results demonstrated the ability of PMP to effectively repair skin wounds in this animal model. These findings serve as compelling evidence for the potential development of PMP-based drugs for wound treatment.

2. Materials and methods

2.1. Materials

Pinctada martensii was provided by Beihai Beishan Pearl Breeding Co.,Ltd. in Guangxi. HSF were purchased from the Cell Bank of the Chinese Academy of Sciences (Shanghai, China). Human Basic fibroblast growth factor was purchased from MedChemExpress (Shanghai, China). In this study, only analytical-grade chemicals were used.

2.2. PMP preparation

The *Pinctada martensii* specimens were collected and carefully washed with water to eliminate any sediment and seaweed adhering to the pearl oyster shells. Next, the closed-shell muscle was dissociated using a scalpel. The *Pinctada martensii* shells were gently pried open, and the protein present on the body surface was extracted using a pasteurized pipette. To remove impurities, the protein was periodically separated using gauze. Subsequently, the filtered protein was subjected to centrifugation at 13,000×*g* for 10 min at 25 °C, and the resulting supernatant, containing the protein of interest, was collected and designated as PMP.

2.3. Cell culture

HSF was grown in DMEM complete medium (Gibco, USA) containing 10 % fetal bovine serum (FBS, Every Green, China). Besides, 100 U/mL penicillin and 100 μg/mL streptomycin (Corning, USA) were added to the culture medium. Cells were kept at 37 °C and 5 % CO_2 in an incubator (Thermo, USA).

2.4. Animals

Thirty-six male rats (approximately 180–200 g) were purchased from the Animal Experiment Center of Guangxi Medical University (China). These animals were housed in a standard laboratory with temperature (24 ± 2 °C) and humidity control (50 ± 10 %) with 12 h light/12 h dark cycle. All animals experiment was approved by the Experimental Animal Care Ethics Committee of Guangxi Medical University (NO. 202205250).

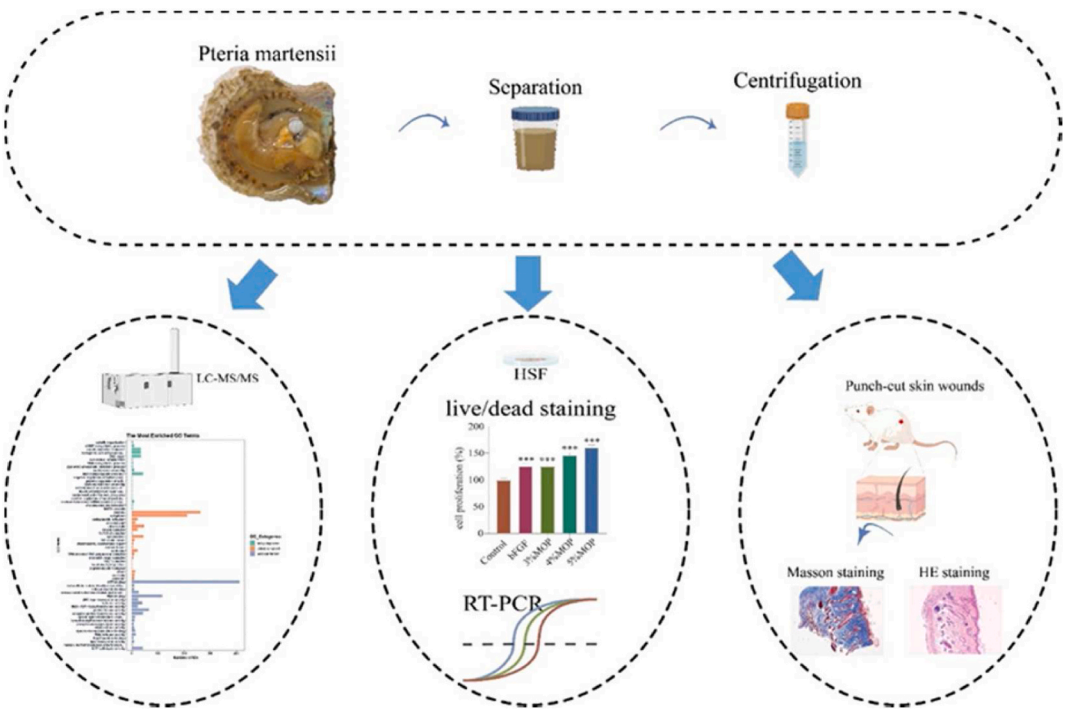

Scheme 1. The native protein was extracted and purified from PMP by filtration and centrifugation, and the composition of PMP was analyzed using LC-MS/MS. In addition, the ability of PMP to promote HSF proliferation and migration in vitro and repair wounds in vivo was detected.

2.5. Cell proliferation assays

To detect the effect of PMP on HSF proliferation, Cell Counting Kit-8 (CCK-8, Biosharp, China) was applied. HSF was grown in culture dishes with a density of 2×10^4 cells per well. The cells were grown in a cell incubator for 24 h. After the cells completely adhered to the wall. 100 μL of serum-free medium with different PMP concentrations (300, 400, and 500 μg/mL) was treated with cells. After co-culture for 24, 48, 72, and 96 h, 100 μL of serum-free medium containing 10 % CCK-8 was added and incubated for another 1 h. The OD value was then measured at a wavelength of 450 nm.

2.6. Scratching experiment

HSF was inoculated in 6-well plates with a density of 6×10^5 cells per well. Cell confluence exceeded 90 %, and the cells were scratched in the six-well plate with a 10 μL gun tip and the scratched cells were removed by washing with PBS. HSF cells were grown in serum-free media containing PMP with a concentration of 500 μg/mL, and pictures of cells were taken at 0, 12, 24, and 36 h after scratching.

2.7. Rat skin trauma model establishment

The rats had their full-thickness back hair, measuring 10 mm in diameter, removed. Subsequently, they were randomly divided into three groups (n = 4): a 100 ng/mL bFGF positive control group, a physiological saline negative control group, and a PMP group treated with 500 μg/mL PMP. Each rat was housed individually in a cage and received a daily application of 20 μl of the respective drug from day 1 to day 14. Rats were anesthetized by intraperitoneal injection of sodium pentobarbital (50 mg/kg). All surgeries were conducted while the animals were under the effect of pentobarbital anesthesia, and utmost efforts were made to minimize any potential suffering experienced by the animals.

2.8. Measurement of wound healing rate

The wound healing rate was detected from the calculated wound area. To accurately record the healing of the wound, the front end of a 20 mL syringe was cut off to form a circular shape with a diameter of 1.8 cm, so as maintain a certain distance between the camera and the wound of rat. The wound area was measured at a fixed height on days 0, 3, 7, 11, and 14 of the experiment. Image J software was utilized to calculate the area. The wound healing rate was calculated as 100 % of the initial (day 0) size of the wound. The wound healing rate was determined as follows: Wound healing rate (%) = (day 0 area - day N area)/day 0 area × 100 % (N = 0, 3, 7, 11, 14). In addition, the wound healing was photographed and recorded.

2.9. Skin tissue acquisition

Rat was sacrificed and 3 mm of tissue around the wounds was collected on day 14. The tissue around each rat wound was removed and immersed in a 4 % paraformaldehyde solution. Then, the skin was dehydrated with a series of increasing concentrations of alcohol (50 %, 70 %, 95 %, and 100 %). The dehydrated tissues were embedded in paraffin to prepare sample sections for the histopathological observation.

2.10. Histological analysis

To observe histopathological changes, sections were stained by H&E and Masson trichrome kits and then examined using an Olympus microscope (Tokyo, Japan) at magnifications of 40, 100, 200, and 400 × . The collagen fiber arrangement was observed. The positive area of collagen fibers in Masson was calculated using Image J software.

2.11. Real-time polymerase chain reaction assay

We purified total RNA from culture cells using a Total RNA kit (Magen, Guangzhou, China). RNA was then synthesized using the cDNA synthesis kit (Takara Bio, Japan). SYBER green quantitative real-time polymerase chain reaction (PCR). Super Mix Plus (Roche, 50,837,000) was utilized to detect the target gene transcript through an RT-PCR system (Roche, Basel, Switzerland). Glyceraldehyde 3-phosphate dehydrogenase (GAPDH) was applied as a control. The procedure consisted of 45 cycles of 95 °C for 10 s and 60 °C for 60 s. Furthermore, the relative expression of target genes was measured by the 2–ΔΔCT method. The sequences of primers used throughout this study are listed in Supplementary Table 1. The total RNA of the cells was extracted with a trizol reagent (Thermo, USA).

2.12. LC-MS/MS analysis

The methods refer to previous literature [30]. 0.1 % formic acid and 2 % acetonitrile were used to dissolve tryptic peptides. A gradient of solvent B (0.1 % formic acid in 90 % acetonitrile) changed from 4 % to 16 % occurred over 38 min, 16 %–30 % in 8 min, and 80 % in 4 min. All samples were run at a constant flow rate of 500 mL/min with an EASY-nLC 1000 UPLC system. A tandem mass spectrometry (MS/MS) in Q ExactiveTM Plus (Thermo) coupled to an online UPLC was performed on these peptides following exposure

to an NSI source. 2.2 kV electrospray voltage was applied. 350–1600 m/z was scanned with Orbitrap, and 7×10^4 intact peptides were detected. An MS/MS analysis using NCE setting 28 was then performed, and fragments were detected using an Orbitrap with a 17, 500-pixel resolution, in which 20 MS/MS scans were conducted with 15.0 s dynamic exclusion and an automatic gain control (AGC) of 5E4 was employed A data-dependent procedure. There was a fixed mass of 100 m/z set as the first mass.

2.13. Databases analysis

Proteome Discoverer (V2.4.1.15) was utilized to process the MS/MS data. Tandem mass spectra against QCP003-uniprot-ompressed-true-download-true-format-fasta-Query-28-28taxon-2022.11.04-08.04.17.05.fasta was searched. Additionally, a reverse decoy database was included to calculate false positive rates. Trypsin/P allows for up to two missing cleavages, and the precursor ions were mass toleranced to 20 ppm in the first search, then 5 ppm in the main search. The mass tolerance for secondary fragment ions was set at 20 PPM. Cys was to be modified by carbamidomethyl, and Met by oxidation. FDRs were adjusted down to 1 %, and minimum peptide scores were set at more than 40.

2.14. Statistical analysis

The experimental data were stated as mean ± standard deviation (mean ± SD). All experimental data were analyzed using

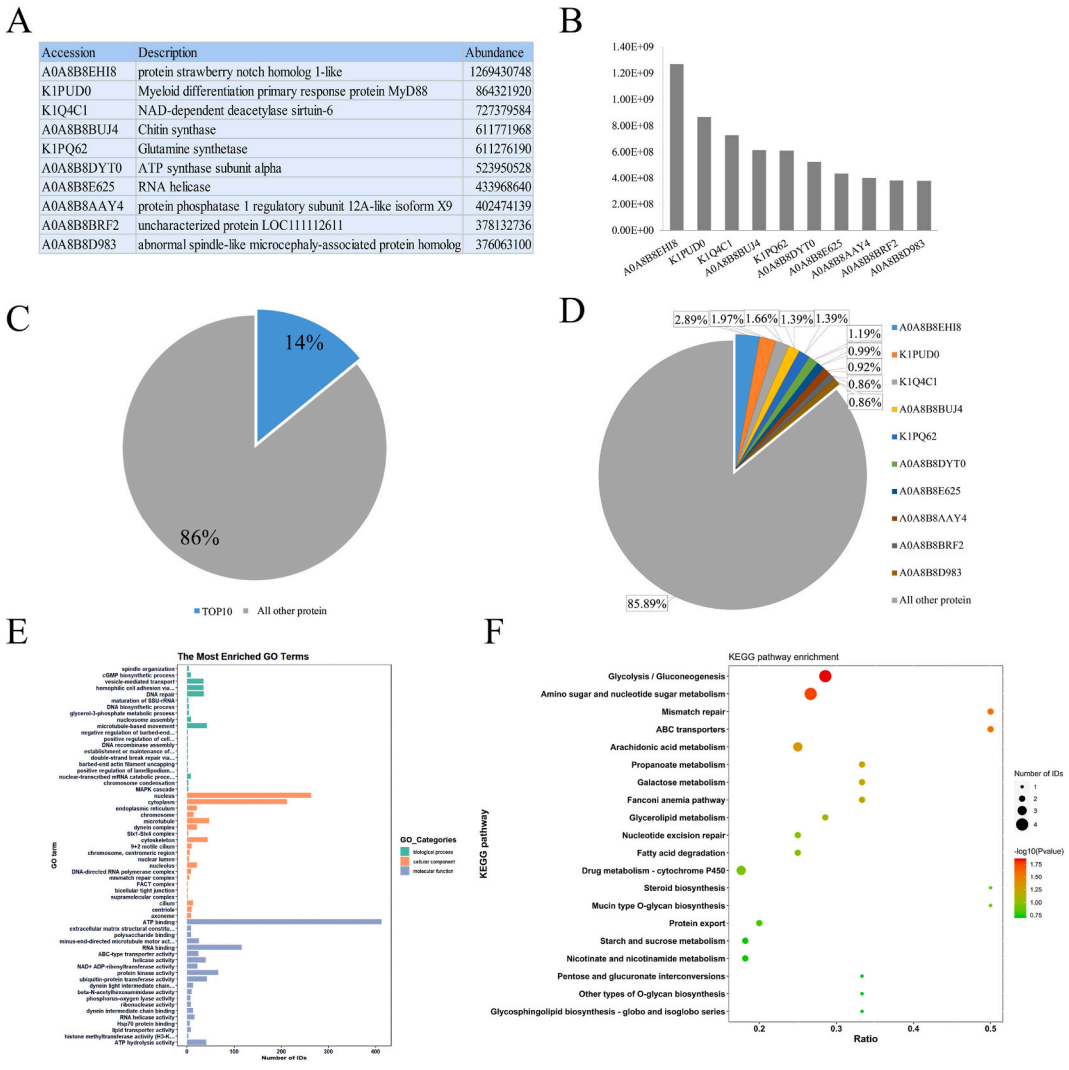

Accession	Description	Abundance
A0A8B8EHI8	protein strawberry notch homolog 1-like	1269430748
K1PUD0	Myeloid differentiation primary response protein MyD88	864321920
K1Q4C1	NAD-dependent deacetylase sirtuin-6	727379584
A0A8B8BUJ4	Chitin synthase	611771968
K1PQ62	Glutamine synthetase	611276190
A0A8B8DYT0	ATP synthase subunit alpha	523950528
A0A8B8E625	RNA helicase	433968640
A0A8B8AAY4	protein phosphatase 1 regulatory subunit 12A-like isoform X9	402474139
A0A8B8BRF2	uncharacterized protein LOC111112611	378132736
A0A8B8D983	abnormal spindle-like microcephaly-associated protein homolog	376063100

Fig. 1. PMP protein abundance and their putative functions. (A) LC–MS/MS Analysis determines the ten most abundant PMP proteins. (B) The ten most abundant PMP proteins were arranged and exhibited by the histogram. (C) The proportion of the ten most abundant PMP proteins in total proteins. (D) The ratio of each of the ten most abundant PMP proteins in total proteins. (E) The enriched GO terms for these proteins by GO analysis. (F) The enriched pathways for these proteins by KEGG pathway analysis.

GraphPad Prism 9.0. Significant differences were analyzed using one-way ANOVA. $p < 0.05$ and $p < 0.01$ were considered statistically significant differences.

3. Result

3.1. Identification of PMP

The protein and abundance of PMP were analyzed utilizing tandem quadrupole liquid chromatography-mass spectrometry (LC-MS/MS). Altogether, a total of 3023 proteins were identified, and the top 10 species with the highest abundance were A0A8B8EHI8, K1PUD0, K1Q4C1, A0A8B8BUJ4, K1PQ62, A0A8B8DYT0, A0A8B8E625, A0A8B8AAY4, A0A8B8AAY4 A0A8B8BRF2 and A0A8B8D983 (Fig. 1A–B). The cumulative abundance of the top ten proteins constituted 14 % of the overall abundance. Among these species, the A0A8B8EHI8 protein accounted for 2.89 %, followed by the K1PUD0 protein (1.97 %) and the K1Q4C1 protein (1.66 %) (Fig. 1C–D). Going to take a further step, the GO and KEGG enrichment analyses were performed to describe the protein functions of PMP. GO enrichment analysis showed that vesicle transport, and cell adhesion involving microtubule-based movement were the highest protein content items in the BP category. For the MF category, the three items with the highest protein content were ATP binding, RNA binding, and protein kinase activity. In the CC category, nuclear, cytoplasmic, and microtubules were the three most important items (Fig. 1E). These results suggested that PMP participates in the regulation of cell division, drives cell migration and orientation, and play an key role in the transportation and localization of intracellular substances [31]. According to KEGG classification analysis, these proteins regulate a variety of signal pathways, including glycolytic glycogenesis, an amino sugar, and nucleotide sugar metabolism (Fig. 1 F).

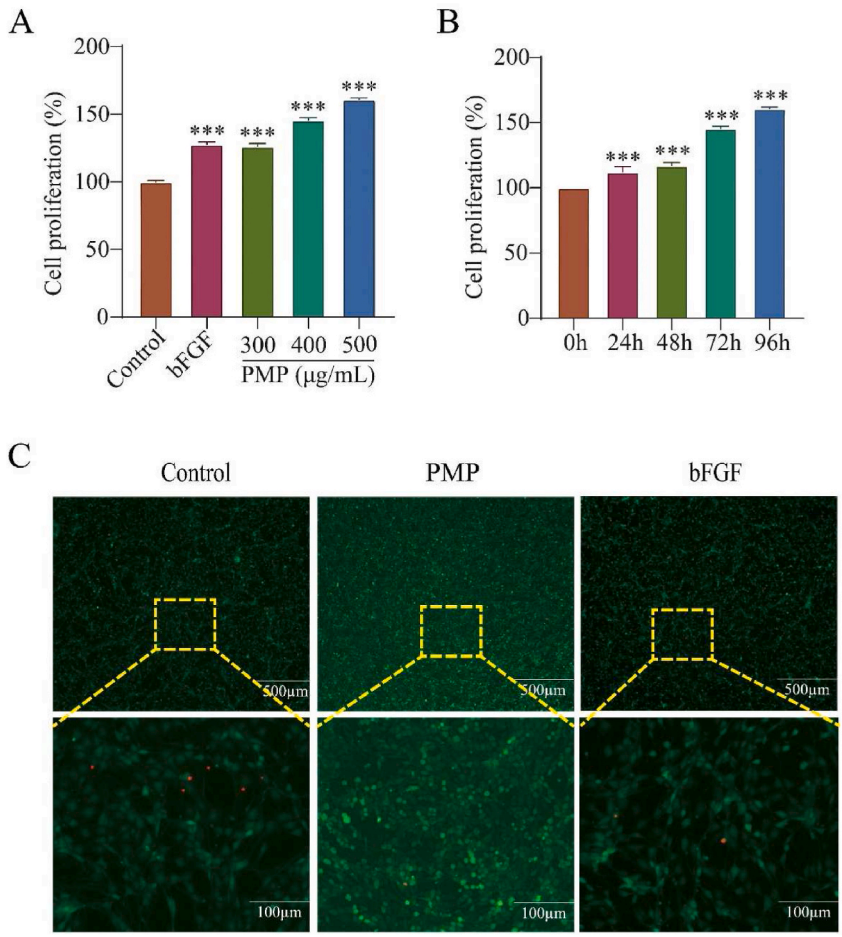

Fig. 2. Effect of PMP on cell proliferation. (A) Effect of different concentrations of PMP on cell proliferation. (B) Effect of 500 μg/mL PMP on cell proliferation at 24, 48, 72, and 96 h. (C) 500 μg/mL PMP in 24h live-dead staining. (n = 4). Note: "*" means significantly different compared with the Control group ($p < 0.05$), "**" means a highly significant difference compared with the Control group ($p < 0.01$), and "***" means a highly significant difference compared with the Control group ($p < 0.001$). The positive Control group was bFGF at a concentration of 100 ng/mL.

3.2. PMP promotes fibroblast proliferation

To determine the proliferation activity of PMP, HSF was incubated with PMP at different concentrations for varying periods, and the cell viability was measured using a CCK-8 kit. bFGF was set as a positive control in this experiment. The results are shown in Fig. 2A, the cell viability was markedly enhanced by 100 ng/mL bFGF for 96 h, and similar results were observed in the PMP-treated group. The cell viability from groups PMP showed enhancement with a dose effect and 300, 400, and 500 μg/mL PMP treated groups were significantly increased by 1.25, 1.46, and 1.6-fold, respectively. Further, in vitro assessment of time-dependent was performed, as shown in Fig. 2B, HSF viability was 1.12-fold higher than that of the control group at 24 h, and increased to 1.6-fold after 96 h. The viability of fibroblasts was also evaluated using a Live/Dead assay kit, green fluorescence represents live cells, while red fluorescence represents dead cells. The result showed that greater cell density and obviously green fluorescence signal were observed after 24 h of the PMP-treated group, while hardly red fluorescence appeared when compared to the control group, which was consistent with the CCK-8 kit detection result (Fig. 2C). The bFGF-treated group also observed similar green fluorescence signal enhancement, yet it was weaker than the PMP-treated group, indicating that PMP effectively promoted HSF proliferation without toxicity. These results suggested that PMP is a potential candidate for promoting wound healing in vivo.

3.3. PMP promotes fibroblast migration

Cell migration is another important process during wound healing. Previous studies have shown that cell migration helps to promoting the closure of open wounds and thus accelerating wound repair. The migration of fibroblasts was examined using a scratch assay. We removed cells and formed a scratch with a diameter of approximately 500 mm, subsequently, cells were treated with PMP or bFGF (set as a positive control). After 12 h post-scratch, the cells in the group treated with PMP exhibited notable movement, and the number of migrated cells was greater compared to the control group. Additionally, we observed that the duration of PMP treatment positively correlated with the extent of cell migration, as evidenced by the nearly complete recovery of the scratch after 36 h (Fig. 3A). Moreover, the migration rate was determined using ImageJ based on cell migration, and the addition of PMP significantly enhanced the migration rate of HSF cells. After 12h, 24h, and 36 h, the cell migration rates were 32.9 %, 52.9 %, and 77.5 %, respectively. And the negative control groups in the same period were 8.1 %, 22.3 %, and 50.5 %, respectively (Fig. 3B). Interestingly, we noted that the cell migration rate in the group treated with 500 μg/mL PMP was marginally higher than that of the group treated with 100 ng/mL bFGF.

3.4. Effect of PMP on gene expression

To better understand how PMP affects the expression of fibroblast genes, 500 μg/mL PMP and HSF co-incubate for 24 h, then the total mRNA of the cell was extracted, and the COL1A1, COL3A1, and MMP-1 genes relative expression levels were determined by qRT-

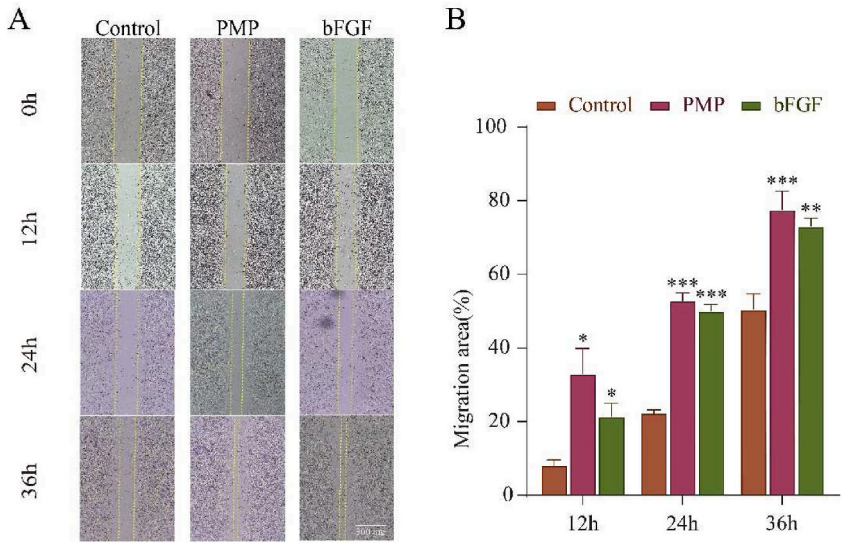

Fig. 3. Effect of PMP on cell migration. (A) In vitro, scratch assay shows that human skin fibroblast cultures appear to migrate at a faster rate after treatment with PMP at a concentration of 500 μg/mL for 12, 24, and 36 h compared to the Control group. (B) Quantification of cell migration rate plots after 12, 24, and 36 h of PMP treatment. The results demonstrate that the largest value of the difference between the migration rates of the groups occurred at 36 h. PMP treatment shortened the in vitro healing time. It exhibited similar cell migration-promoting effects as growth factors. (n = 3). Note: "*" means significantly different compared with the Control group ($p < 0.05$), and "**" means a highly significant difference compared with the Control group ($p < 0.01$), and "***" means a highly significant difference compared with the Control group ($p < 0.001$). The positive Control group was bFGF at a concentration of 100 ng/mL.

PCR. Fig. 4A presents the results derived from the preliminary analysis of qRT-PCR. The COL1A1 expression level of the PMP-treated group was observed to be approximately 1.73-fold higher than that of the control group. Conversely, the COL1A1 expression level of the bFGF-treated group was found to be reduced by approximately 80 % compared to the control group, suggesting that PMP and bFGF may promote cell proliferation and migration through distinct mechanisms. The results of the COL3A1 assay were consistent with those of the COL1A1 assay (Fig. 4B), as PMP was found to increase the expression level of the COL3A1 gene. Furthermore, both the PMP- and bFGF- treated groups exhibited an approximately 1.66 and 1.68-fold increase in MMP-1 gene expression compared to the control group, respectively (Fig. 4C).

3.5. In vivo assay of the effect of PMP on wound healing

Inspired by the significant cell proliferation and migration observed in vitro with PMP, we conducted further experiments to evaluate its effectiveness in wound repair using a full-thickness excisional wounding model in SD rats. As shown in Fig. 5A, two wounds with a diameter of about 10 mm were created on the rats, and PMP was uniformly applied to the wounds every day. The wound diameter was measured by vertical isometric photography on days 0, 3, 7, 11, and 14. As shown in Fig. 5B, on the third day after treatment, all groups showed reduced wound areas. However, the PMP and bFGF-treated groups exhibited smaller areas compared to the control group. This difference became more pronounced on the 7th day of treatment. Importantly, in the PMP-treated group, the wound surface was covered by new epidermis, and there was de novo hair regeneration, indicating that the skin healing in this group was a result of cell proliferation and migration rather than self-contraction of the wound. By the 14th day, the wounds in the PMP-treated group were almost completely healed, while the wound in the blank control group remained open. To further quantify the wound healing process, we developed a digital model.

As shown in Fig. 5C–E, the wound healing rates of the PMP and bFGF-treated rats were 52.09 % and 55.78 % on day 3, respectively, which were significantly higher than that of the blank control group (30.48 %). By day 7, the wound healing rate in the PMP-treated group reached 87.45 %, which was approximately 20 % higher than that of the blank control group. On day 14, when the control group were sacrificed, a large area of red color was still visible in the middle of the wound, indicating incomplete healing. However, the wound healing rates of the PMP and bFGF-treated groups reached 99.89 % and 99.60 %, respectively. These results suggest that PMP application promotes wound healing in vivo. The PMP-treated group showed accelerated wound closure, new epidermis formation, and hair regeneration compared to the control group. The wound healing rates were consistently higher in the PMP and bFGF-treated groups throughout the experimental period, indicating the potential therapeutic efficacy of PMP in wound repair.

3.6. Analysis of H&E and Masson staining

To examine the pathological changes in the skin tissue, histological sections of the newly formed skin were stained with H&E and evaluated. As shown in Fig. 6A, skin structures at various scales (40 × , 100 × , 200 × , 400 ×) were observed with different treatments. Normal skin exhibited a well-structured epidermis, dermis, and subcutaneous tissues. The isolated epidermis appeared elastic and wavy, while the dermis contained various skin appendages such as hair follicles and sweat glands. The connective tissue was evenly distributed, and the subcutaneous tissue had a rich fat layer.

However, the blank control group showed unsatisfactory structural recovery in wound repair. The epidermis was thick, and its keratinization was immature. A crust remained unexfoliated in the center of the wound, and the epithelial cell layer beneath the crust did not meet properly, while the PMP-treated group exhibits a notable capability to decrease dermal thickness and concurrently enhance epidermal thickness significantly (Fig. 6B–C). Additionally, no regeneration of skin appendages was observed in the dermis

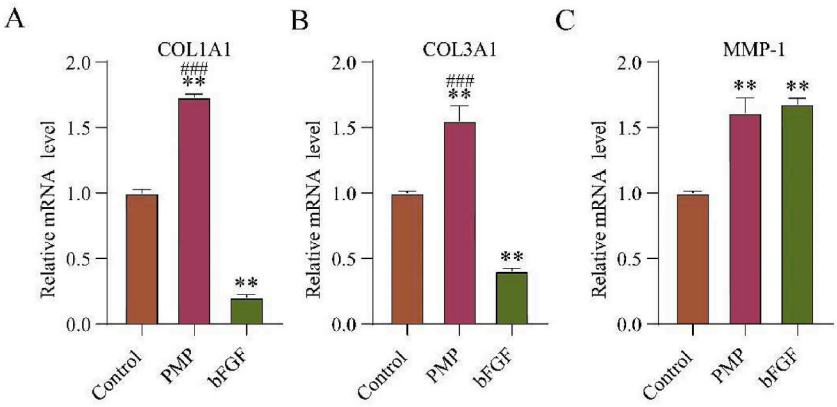

Fig. 4. Effect of PMP on gene expression in human skin fibroblasts. RT-PCR was performed to detect mRNA expression, and the test showed that after 24 h of treatment with PMP at a concentration of 500 μg/mL, the expression of (A) COL1A1, (B) COL3A1, and (C) MMP-1 collagen-related mRNA was up-regulated. (n = 3). Note: "*" means significantly different compared with the Control group ($p < 0.05$), and "**" means a highly significant difference compared with the Control group ($p < 0.01$). "###" means significantly different compared with the bFGF group ($p < 0.01$).

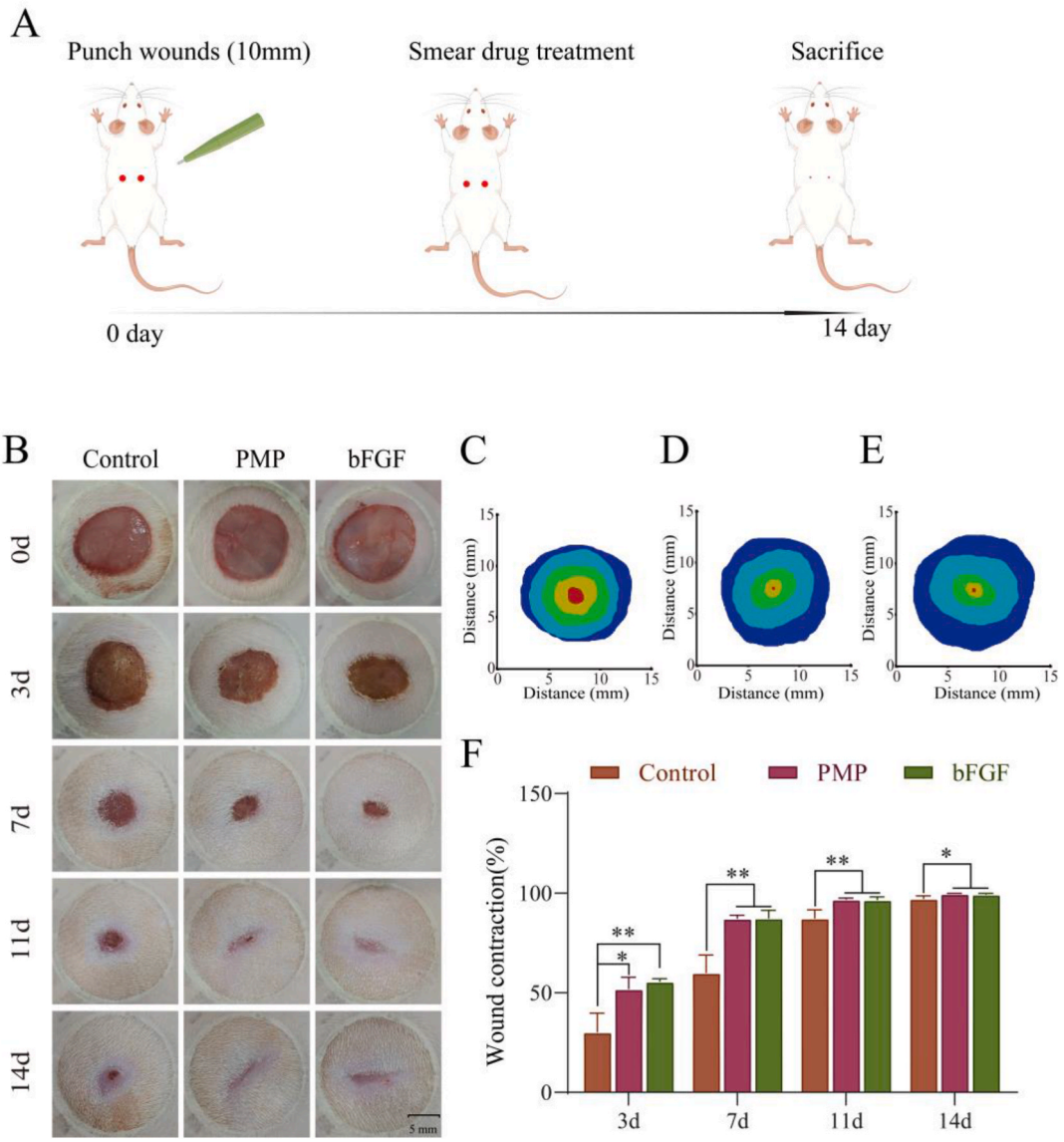

Fig. 5. Macroscopic assessment of wound healing progression. (A) Pattern diagram of the rat wound repair model. (B) Wound appearance. Wound areas of Control (NaCl: 0.9 %) and PMP-treated groups at 3, 7, 11, and 14d after injury. Quantification of the wound area in the (C) Control, (D) PMP, and (E) bFGF groups, respectively. (F) Quantitative measurement of wound healing area. Note: "*" and "**" means significantly different. (n = 4).

(Fig. 7A). In comparison, the PMP and bFGF-treated groups exhibited better reconstruction of skin appendages. On day 14, the PMP-treated group presented the thinnest, flat, and smooth epidermis. The subcutaneous appendages and collagen fibers were tightly arranged and orderly, indicating that PMP significantly promoted fibroblast proliferation and re-epithelialization at the wound site. This resulted in a faster wound repair rate and improved healing effect, enhancing the skin's healing ability (Fig. 7B–C). The bFGF-treated group also showed better repair of the dermis and epidermis. Additionally, Masson staining of skin tissue sections on day 14 was performed. The staining results revealed a greater presence of collagen fibers (blue) in the PMP-treated group compared to the control and bFGF-treated groups (Fig. 7C), which aligned with the PCR results (Fig. 5A and C). The distribution of collagen in the PMP-treated group was uniform and more intact, indicating that PMP promoted wound healing by stimulating collagen production and deposition. Further analysis of cutaneous appendages in the regenerated skin also demonstrated a higher number of appendages compared to the control group (Fig. 7B).

4. Discussion

Wound healing is a complex biological process consisting of four overlapping phases: coagulation, inflammation, migration and

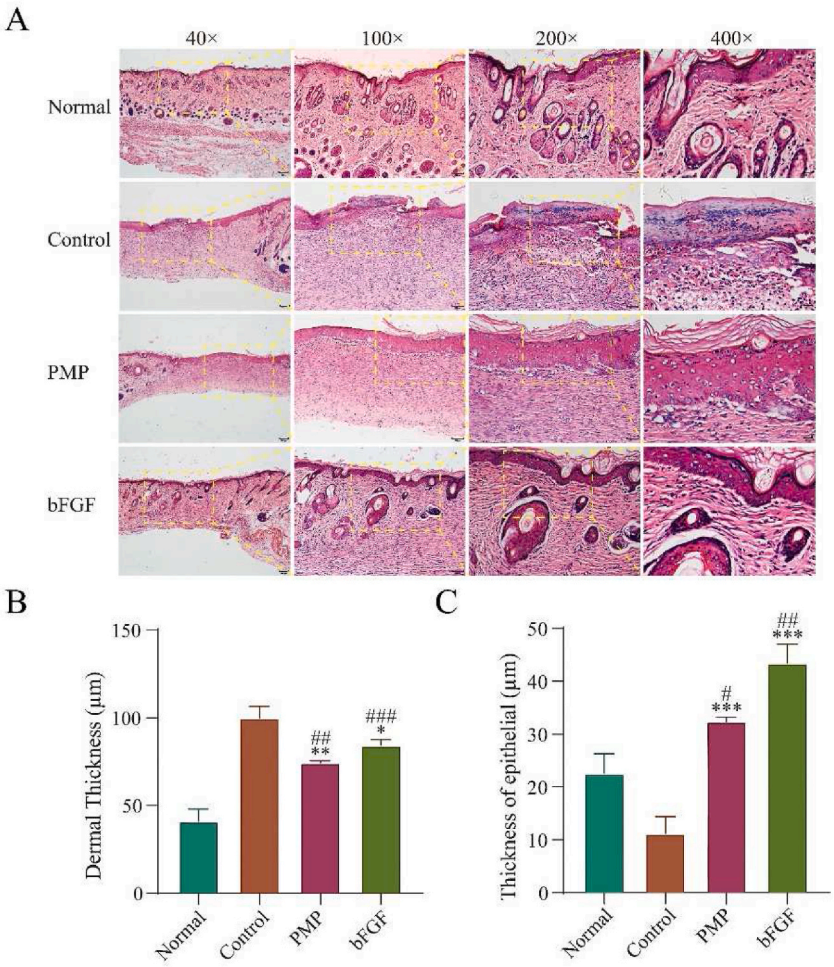

Fig. 6. Histological evaluation of the evolution of wound healing. (A) Histological characteristics of the injured tissue. The top panel shows representative features of normal rat skin under H&E staining. Images obtained in light microscopy (40 × , 100 × , 200 × , and 400 × magnifications). (B) The thickness of the dermis was selected as the evaluation index. (C) The thickness of the epidermal layer was chosen as the evaluation index. (n = 4). Day 14 post-injury. Analysis was performed using ImageJ® software. Note: "*" means significantly different compared with the Control group ($p < 0.05$), "**" means a highly significant difference compared with the Control group ($p < 0.01$), and "***" means a highly significant difference compared with the Control group ($p < 0.001$). "#" means significantly different compared with the normal group ($p < 0.05$), and "###" means a highly significant difference compared with the normal group ($p < 0.01$).

proliferation, and remodeling [12]. Abnormal wound healing can lead to chronic wounds or incomplete skin structure [32], imposing a significant burden on patients and the healthcare system [6]. Therefore, it is crucial to develop effictive drugs or products for high-quality wound healing treatment. Taking inspiration from the intricate mechanism of self-injury repair involved in the formation of pearls by PM [33], we extracted its secreted protein, isolated and purified it to obtain PMP. We demonstrated in vitro that PMP exhibited a dose- and time-dependent manner ability to promote cell proliferation and migration (Fig. 2). The promotion of cell proliferation by PMP may be attributed to its specific protein composition (Fig. 1A). To further evaluate the efficacy of PMP, we utilized a full-thickness skin model in rats and observed that PMP accelerated wound healing, consistent with the in vitro results. This beneficial effect may be attributed to the enhancement of collagen metabolism and fibroblast proliferation. Importantly, our study focused on the activity of natural proteins extracted from PM, as opposed to their enzymatic hydrolysates, which distinguishes it from existing research [29].

As far as we know, the protein secreted by PM is often regarded as waste. Few studies have focused on detecting its biological activity. Exploring its repair activity in skin tissue will not only improve the utilization value of PM but also protect the environment.

An interesting result in the assay of cellular gene expression was found: PMP increased the expression of COL1A1 (type I collagen) and COL3A1 (type III collagen) compared to the PBS-treated group, while bFGF treatment inhibited the expression of both these genes. This suggests that PMP may play a different mechanism than bFGF in wound repair [13,34,35]. Type Collagen I has a coarse structure and hard texture, which helps with epithelial cell proliferation and promotes collagenase production. This contributes to skin tone and elasticity [36]. Type III collagen fibers have smaller and more elastic structures with less abundance in the skin. They play a role in

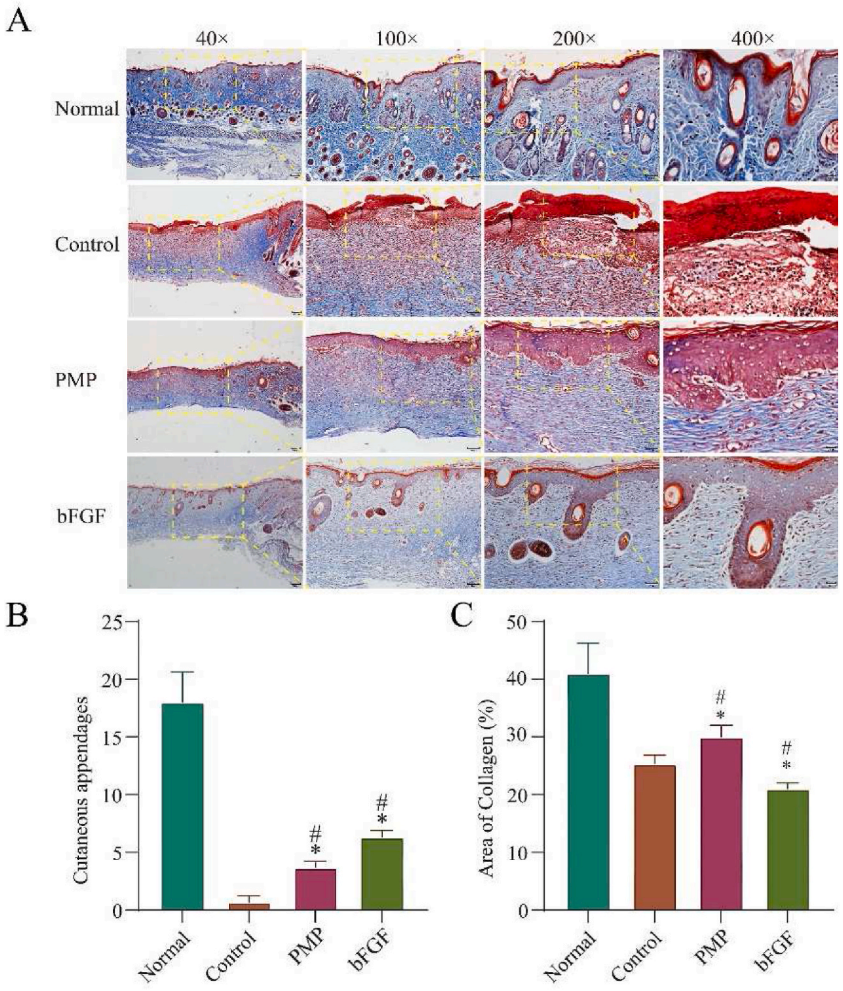

Fig. 7. Masson trichrome staining shows the histology of the repaired wounds. (A) Normal skin tissue structure with the saline, PMP, and bFGF groups 14 days after surgery. (B) Number of skin appendages. (C) Area of collagen in skin tissues. (n = 4). Note: "*" means significantly different compared with the Control group ($p < 0.05$). "#" means significantly different compared with the normal group ($p < 0.05$).

strengthening microvessels, providing nutrients to cells, and promoting the formation of new blood vessels [37]. During tissue remodeling, metalloproteinases secreted by macrophages degrade excess fibers in wounds, induce apoptosis and removal of fibroblasts, and promote scar reduction [38]. The up-regulation of type III collagen synthesis during the proliferation phase is beneficial for reducing scar formation [12,39,40].

The administration of PMP resulted in smooth new skin tissue and no scar formation, likely due to the promotion of cellular type III collagen expression. Additionally, H&E staining showed that PMP effectively accelerated wound epithelialization compared to the control group (Fig. 6A), correlating with its significant promotion of cell migration. Masson staining also demonstrated the potential of PMP in wound healing treatment (Fig. 7 A). These findings highlight the potential of PMP in the treatment of wound healing, as it is closely associated with promoting cell migration, collagen deposition, and remodeling of collagen fibers. The biological activity of PMP in promoting wound healing has been demonstrated. However, the specific active protein(s) involved are still not clear and require further research. Fortunately, the composition of PMP has been identified, which provides a clear formula for future screening and wound repair purposes.

Since PMP has been identified as a potential candidate for wound treatment, our study aimed to gain insight into its active substances. To identify the main protein components of PMP, we conducted proteomic analysis. This analysis provided a theoretical basis for further investigation into the specific functional proteins in PMP.

Interestingly, among the proteins found in high abundance, we discovered an immunomodulation protein (K1PUD0, MyD88). MyD88 acts as a key bridging molecule for IL-1 and Toll-like receptor (TLR) signaling pathways [41]. It is well-known that TLR is a family of pattern recognition receptors that recognize various pathogen-associated molecular patterns (PAMPs) and activate innate immune defenses against pathogen invasion [42,43]. Previous studies have shown that MyD88 can mediate cell proliferation and migration by activating the NF-κB/AP-1 signaling pathway [41].

Additionally, we identified another highly abundant protein, chitin synthase (A0A8B8BUJ4). Its presence suggests that PMP contains precursor substances and possible product formation for catalyzing the synthesis of chitin. Numerous reports have demonstrated the accelerating effects of chitin and its derivatives on wound healing [44]. Furthermore, we found another highly abundant protein, glutamine synthetase (K1PQ62), which has been reported to promote satellite cell and muscle regeneration through macrophage-derived glutamine [45]. According to the KEGG analysis, these proteins are mainly involved in glycolytic glycogenesis, amino saccharide, and nucleotide glycolysis processes. For cells in the proliferative phase, glucose uptake not only provides ATP energy but also serves as an important carbon source for synthesizing lipids and non-essential amino acids, supporting cell growth [46]. During skin wound healing, PMP may regulate the rate of glucose uptake by cells through its multiple epidermal growth factor analogs, thereby promoting cellular metabolism and faster cell proliferation. In conclusion, our findings shed light on the active substances present in PMP. The identification of immunomodulation proteins, chitin synthase, and glutamine synthetase provides valuable insights into the potential mechanisms underlying PMP's role in wound healing. Further research is warranted to explore the specific functions and therapeutic applications of these proteins in wound repair.

5. Conclusion

In summary, we collected pearl mussel protein from waste materials and obtained PMP through filtration and centrifugation processes. By identifying the major components of PMP, we gained insight into its composition, which includes a variety of active proteins such as epidermal growth factor-like proteins, immune regulatory proteins, and various enzymes. Our research indicated that PMP has the potential to promote fibroblast migration and proliferation. We observed an upregulation of gene expression levels related to collagen (COL1A1, COL3A1) and MMP-1 in HSF treated with PMP. This suggests that PMP may have the ability to reduce scar formation in damaged skin. Furthermore, further studies conducted in vivo confirmed the beneficial effects of PMP on wound healing. Wounds treated with PMP showed significant improvements, including normalized dermal structure, increased collagen fiber content, and the formation of a mature epidermal layer. Based on these findings, it can be concluded that PMP derived from marine sources holds promise as a potential candidate for further investigation into its role in wound healing.

Institutional review board statement

Not applicable.

Data availability statement

The data presented in this study are available in the article.

Ethics statement

This study was reviewed and approved by the Experimental Animal Care Ethics Committee of Guangxi Medical University, with the approval number: NO. 202205250. Animal studies were conducted in compliance with the Animal Research: Reporting of In Vivo Experiments (ARRIVE) guidelines [47]. All the studies were performed in accordance with relevant guidelines and regulations.

CRediT authorship contribution statement

Tao Zeng: Data curation, Investigation, Methodology, Writing – original draft. **Lianfeng Liu:** Data curation, Investigation, Methodology. **Dandan Mo:** Methodology. **Qinghua Yang:** Writing – original draft. **Xiaohao Hu:** Methodology. **Chun Lu:** Data curation. **Ran Sun:** Writing – original draft. **Li Zheng:** Funding acquisition, Supervision, Writing – review & editing. **Bo Zhou:** Funding acquisition, Supervision, Writing – review & editing. **Sheng Xu:** Investigation, Methodology, Supervision, Writing – original draft, Writing – review & editing.

Declaration of competing interest

The authors declare that they have no known competing financial interests or personal relationships that could have appeared to influence the work reported in this paper.

Acknowledgments

This work was supported by the Guangxi Scientific Research and Technological Development Foundation (Grant No. GuikeAB21220062), the Guangxi Science and Technology Major Project (Grant No. GuikeAA19254002), China Central Guiding Local Science and Technology Development Fund Projects of Nanning (Grant No. 20233013).

Appendix A. Supplementary data

Supplementary data to this article can be found online at https://doi.org/10.1016/j.heliyon.2024.e24239.

References

[1] H.Q. Lu, J.Y. Yang, Y.J. Cong, Y.X. Xiao, L.Y. Zhang, The comparison of medicinal value of pearl powder and pearl layer powd er, Nat. Prod. Res. Dev. (3) (1991) 35–42.

[2] X. Zhang, C. Hu, Y. Yan, H.F. Yang, J.F. Li, H. Bai, G.C. Xi, J. Liao, Identification of pearl powder using microscopic infrared reflectance spectroscopy, Spectrosc Spect Anal 34 (2014) 2424–2428, https://doi.org/10.3964/j.issn.1000-0593(2014)09-2424-05.

[3] C. Jin, H.Y. Ren, J.W. Pu, X.J. Liu, J.L. Li, Identification of nacre matrix protein genes hic 14 and hic19 and their roles in crystal growth and pearl formation in the mussel Hyriopsis cumingii, Biotechnol Appl Bioc 66 (2019) 545–554, https://doi.org/10.1002/bab.1752.

[4] Y. Sato, A. Komaru, Pearl formation in the Japanese pearl oyster (Pinctada fucata) by CaCO3 polymorphs: pearl quality-specific biomineralization processes and their similarity to shell regeneration, Aquac Res 50 (2019) 1710–1717, https://doi.org/10.1111/are.14057.

[5] R.L. Gallo, T. Nakatsuji, Microbial symbiosis with the innate immune defense system of the skin, J. Invest. Dermatol. 131 (2011) 1974–1980, https://doi.org/10.1038/jid.2011.182.

[6] C. Sen, G. Gordillo, M. Longaker, Human skin wounds: a major and snowballing threat to public health and the economy 17 (2009) 763–771.

[7] C.K. Sen, Human wounds and its burden: an updated compendium of estimates, Adv. Wound Care 8 (2019) 39–48, https://doi.org/10.1089/wound.2019.0946.

[8] L.E. Tracy, R.A. Minasian, E.J. Caterson, Extracellular matrix and dermal fibroblast function in the healing wound, Adv. Wound Care 5 (2016) 119–136, https://doi.org/10.1089/wound.2014.0561.

[9] P. Bainbridge, Wound healing and the role of fibroblasts, J. Wound Care 22 (2013), https://doi.org/10.12968/jowc.2013.22.8.407, 407-408, 410-412.

[10] A. Sonoki, Y. Okano, Y. Yoshitake, Dermal fibroblasts can activate matrix metalloproteinase-1 independent of keratinocytes via plasmin in a 3D collagen model, Exp. Dermatol. 27 (2018) 520–525, https://doi.org/10.1111/exd.13522.

[11] H.E. Talbott, S. Mascharak, M. Griffin, D.C. Wan, M.T. Longaker, Wound healing, fibroblast heterogeneity, and fibrosis, Cell Stem Cell 29 (2022) 1161–1180, https://doi.org/10.1016/j.stem.2022.07.006.

[12] S. Eming, P. Martin, M. Tomic-Canic, Wound Repair Regen.: Mechanisms, signaling, and translation 6 (2014).

[13] P. Wang, B. Shu, Y. Xu, J. Zhu, J. Liu, Z. Zhou, L. Chen, J. Zhao, X. Liu, S. Qi, et al., Basic fibroblast growth factor reduces scar by inhibiting the differentiation of epidermal stem cells to myofibroblasts via the Notch 1/Jagged 1 pathway, Stem Cell Res. Ther. 8 (2017) 114, https://doi.org/10.1186/s13287-017-0549-7.

[14] L. Benington, G. Rajan, C. Locher, L.Y. Lim, Fibroblast growth factor 2-A review of stabilisation approaches for clinical applications, Pharmaceutics 12 (2020), https://doi.org/10.3390/pharmaceutics12060508.

[15] I. Ding, A.M. Peterson, Half-life modeling of basic fibroblast growth factor released from growth factor-eluting polyelectrolyte multilayers, Sci. Rep. 11 (2021) 9808, https://doi.org/10.1038/s41598-021-89229-w.

[16] W.W. Zhang, Y.F. Wei, X.X. Cao, K.X. Guo, Q.Q. Wang, X.C. Xiao, X.F. Zhai, D.D. Wang, Z.B. Huang, Enzymatic preparation of Crassostrea oyster peptides and their promoting effect on male hormone production, J. Ethnopharmacol. (2021) 264, https://doi.org/10.1016/j.jep.2020.113382. ARTN 113382.

[17] C.R. Bakshani, A.L. Morales-Garcia, M. Althaus, M.D. Wilcox, J.P. Pearson, J.C. Bythell, J.G. Burgess, Evolutionary conservation of the antimicrobial function of mucus: a first defence against infection, NPJ Biofilms Microbiomes 4 (2018) 14, https://doi.org/10.1038/s41522-018-0057-2.

[18] H. Okella, H. Ikiriza, S. Ochwo, C.O. Ajayi, C. Ndekezi, J. Nkamwesiga, B. Kaggwa, J. Aber, A.G. Mtewa, T.K. Koffi, et al., Identification of antimicrobial peptides isolated from the skin mucus of african catfish, Clarias gariepinus (burchell, 1822), Front. Microbiol. 12 (2021) 794631, https://doi.org/10.3389/fmicb.2021.794631.

[19] Z. Ye, X. Zhou, X. Xi, Y. Zai, M. Zhou, X. Chen, C. Ma, T. Chen, L. Wang, H.F. Kwok, In vitro & in vivo studies on identifying and designing temporin-1CEh from the skin secretion of Rana chensinensis as the optimised antibacterial prototype drug, Pharmaceutics 14 (2022), https://doi.org/10.3390/pharmaceutics14030604.

[20] Y. Wu, R. Li, J. Ma, M. Zhou, L. Wang, T.I. McClure, J. Cai, T. Chen, C. Shaw, Ranachensinin: a novel aliphatic tachykinin from the skin secretion of the Chinese brown frog, Rana chensinensis, Protein Pept. Lett. 20 (2013) 1217–1224, https://doi.org/10.2174/0929866511320110005.

[21] L.L. Jin, S.S. Song, Q. Li, Y.H. Chen, Q.Y. Wang, S.T. Hou, Identification and characterisation of a novel antimicrobial polypeptide from the skin secretion of a Chinese frog (Rana chensinensis), Int. J. Antimicrob. Agents 33 (2009) 538–542, https://doi.org/10.1016/j.ijantimicag.2008.11.010.

[22] M. McDermott, A.R. Cerullo, J. Parziale, E. Achrak, S. Sultana, J. Ferd, S. Samad, W. Deng, A.B. Braunschweig, M. Holford, Advancing discovery of snail mucins function and application, Front. Bioeng. Biotechnol. 9 (2021) 734023, https://doi.org/10.3389/fbioe.2021.734023.

[23] T. Deng, D. Gao, X. Song, Z. Zhou, L. Zhou, M. Tao, Z. Jiang, L. Yang, L. Luo, A. Zhou, et al., A natural biological adhesive from snail mucus for wound repair, Nat. Commun. 14 (2023) 396, https://doi.org/10.1038/s41467-023-35907-4.

[24] V. Gentili, D. Bortolotti, M. Benedusi, A. Alogna, A. Fantinati, A. Guiotto, G. Turrin, C. Cervellati, C. Trapella, R. Rizzo, et al., HelixComplex snail mucus as a potential technology against O3 induced skin damage, PLoS One 15 (2020) e0229613, https://doi.org/10.1371/journal.pone.0229613.

[25] Z.F. Gu, Q.Y. Wang, J. Fang, N.H. Ye, Y.Z. Mao, Y.H. Shi, Y. Wang, A.M. Wang, Growth of cultured pearl oyster (Pinctada martensii) in Li'an lacoon, hainan island, China, J. Shellfish Res. 28 (2009) 465–470, https://doi.org/10.2983/035.028.0307.

[26] P.T. Huang, J.Y. Miao, J.L. Li, Y.K. Li, X.H. Wang, Y. Yu, Y. Cao, Novel antioxidant peptides from pearl shell meat hydrolysate and their antioxidant activity mechanism, Molecules 28 (2023), https://doi.org/10.3390/molecules28020864. ARTN 864.

[27] M.F. Wei, H.M. Qiu, J. Zhou, C.H. Yang, Y.F. Chen, L.J. You, The anti-photoaging activity of peptides from Pinctada martensii meat, Mar. Drugs 20 (2022), https://doi.org/10.3390/md20120770. ARTN 770.

[28] C. Shen, Z. Guo, H. Liang, M. Zhang, Preliminary investigation of the immune activity of PmH2A-derived antimicrobial peptides from the pearl oyster Pinctada fucata martensii, Fish Shellfish Immunol. 135 (2023) 108691, https://doi.org/10.1016/j.fsi.2023.108691.

[29] T. Zhang, F. Yang, X. Qin, X. Yang, C. Zhang, Z. Wan, H. Lin, Investigation of the in vivo, in vitro, and in silico wound healing potential of Pinctada martensii purified peptides, Mar. Drugs 20 (2022) 417, https://doi.org/10.3390/md20070417.

[30] K. Li, G. Yan, H. Huang, M. Zheng, K. Ma, X. Cui, D. Lu, L. Zheng, B. Zhu, J. Cheng, et al., Anti-inflammatory and immunomodulatory effects of the extracellular vesicles derived from human umbilical cord mesenchymal stem cells on osteoarthritis via M2 macrophages, J Nanobiotechnology 20 (2022) 38, https://doi.org/10.1186/s12951-021-01236-1.

[31] J. Salogiannis, S.L. Reck-Peterson, Hitchhiking: a non-canonical mode of microtubule-based transport, Trends Cell Biol. 27 (2017) 141–150, https://doi.org/10.1016/j.tcb.2016.09.005.

[32] H.N. Wilkinson, M.J. Hardman, Wound healing: cellular mechanisms and pathological outcomes, Open biology 10 (2020) 200223, https://doi.org/10.1098/rsob.200223.

[33] C. Fan, X.K. Zhang, L.M. Tang, X.Z. Zhang, J.L. Li, Y.C. Li, Q.Z. Li, Z.P. Wang, Study on the effect of mass selection and hybridization on growth performance of Chinese pearl oyster Pinctada martensii, Front. Mar. Sci. 9 (2022), https://doi.org/10.3389/fmars.2022.851142. ARTN 851142.

[34] Y. Koike, M. Yozaki, A. Utani, H. Murota, Fibroblast growth factor 2 accelerates the epithelial-mesenchymal transition in keratinocytes during wound healing process, Sci. Rep. 10 (2020) 18545, https://doi.org/10.1038/s41598-020-75584-7.

[35] K. Hishida, S. Hatano, H. Furukawa, K. Yokoo, H. Watanabe, Effects of fibroblast growth factor 2 on burn injury and repair process: analysis using a refined mouse model, Plast Reconstr Surg Glob Open 8 (2020) e2757, https://doi.org/10.1097/GOX.0000000000002757.

[36] M.A. Karsdal, S.H. Nielsen, D.J. Leeming, L.L. Langholm, M.J. Nielsen, T. Manon-Jensen, A. Siebuhr, N.S. Gudmann, S. Ronnow, J.M. Sand, et al., The good and the bad collagens of fibrosis - their role in signaling and organ function, Adv. Drug Deliv. Rev. 121 (2017) 43–56, https://doi.org/10.1016/j.addr.2017.07.014.

[37] D. Singh, V. Rai, D.K. Agrawal, Regulation of collagen I and collagen III in tissue injury and regeneration, Cardiol Cardiovasc Med 7 (2023) 5–16, https://doi.org/10.26502/fccm.92920302.

[38] X. Wang, R.A. Khalil, Matrix metalloproteinases, vascular remodeling, and vascular disease, Adv. Pharmacol. 81 (2018) 241–330, https://doi.org/10.1016/bs.apha.2017.08.002.

[39] R.B. Diller, A.J. Tabor, The role of the extracellular matrix (ECM) in wound healing: a review, Biomimetics 7 (2022) 87, https://doi.org/10.3390/biomimetics7030087.

[40] S. Mathew-Steiner, S. Roy, C. Sen, Collagen in Wound Healing 8 (2021).
[41] G. Zhu, Z. Cheng, Y. Huang, W. Zheng, S. Yang, C. Lin, J. Ye, MyD88 mediates colorectal cancer cell proliferation, migration and invasion via NF-κB/AP-1 signaling pathway, Int. J. Mol. Med. (2019) 131–140, https://doi.org/10.3892/ijmm.2019.4390.
[42] W. Hu, L. van Steijn, C. Li, F.J. Verbeek, L. Cao, R.M.H. Merks, H.P. Spaink, A novel function of TLR2 and MyD88 in the regulation of leukocyte cell migration behavior during wounding in zebrafish larvae, Front. Cell Dev. Biol. 9 (2021) 624571, https://doi.org/10.3389/fcell.2021.624571.
[43] D.Y. Li, M.H. Wu, Pattern recognition receptors in health and diseases, Signal Transduct Tar 6 (2021), https://doi.org/10.1038/s41392-021-00687-0. ARTN 291.
[44] S. Anil, Potential medical applications of chitooligosaccharides, Polymers 14 (2022) 3558, https://doi.org/10.3390/polym14173558.
[45] M. Shang, F. Cappellesso, R. Amorim, J. Serneels, F. Virga, G. Eelen, S. Carobbio, M.Y. Rincon, P. Maechler, K.D. Bock, et al., Macrophage-derived glutamine boosts satellite cells and muscle regeneration, Nature 587 (2020) 626–631, https://doi.org/10.1038/s41586-020-2857-9.
[46] R.J. Myers, Y. Fichman, G. Stacey, R. Mittler, Extracellular ATP plays an important role in systemic wound response activation, Plant Physiol 189 (2022) 1314–1325, https://doi.org/10.1093/plphys/kiac148.
[47] J.C. McGrath, E. Lilley, Implementing guidelines on reporting research using animals (ARRIVE etc.): new requirements for publication in BJP, Brit J Pharmacol 172 (2015) 3189–3193, https://doi.org/10.1111/bph.12955.